Structural diversity in binary superlattices from Au and γ-Fe_2O_3 nanocrystals: towards fine tuning of dipolar interactions

Suyeon Lee[1], Anh-Tu Ngo[1], Isabelle Lisiecki[1]* and Alexa Courty[1]*

1-Sorbonne Université, MONARIS, UMR8233, UMR 8233, F-75005 Paris, France

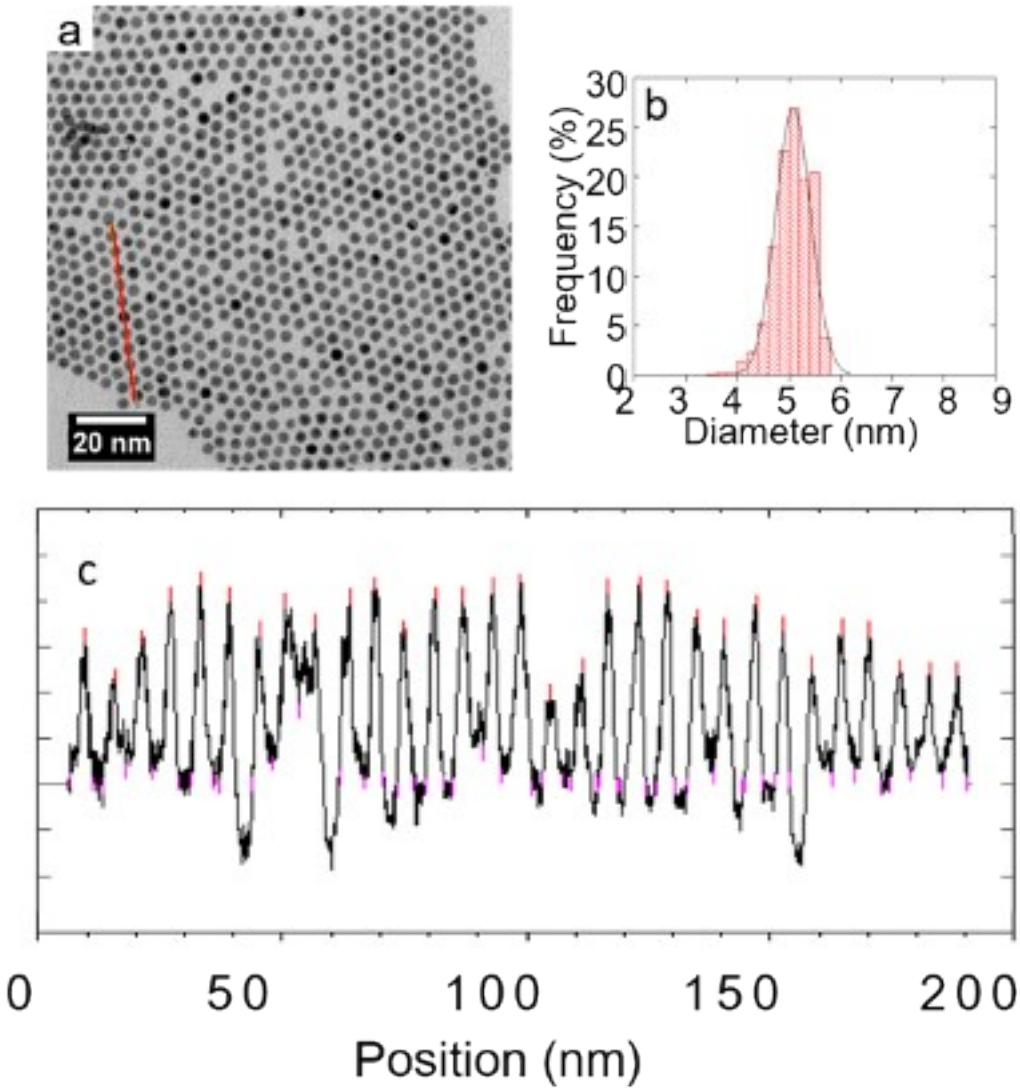

Figure S1. a) TEM image of 4.6 ± 0.3 nm Au NPs , b) corresponding size distribution and c) contrast profile made over the red line allowing to determine the effective diameter $D_{C\text{-}C} \approx 6.4$ *nm.*

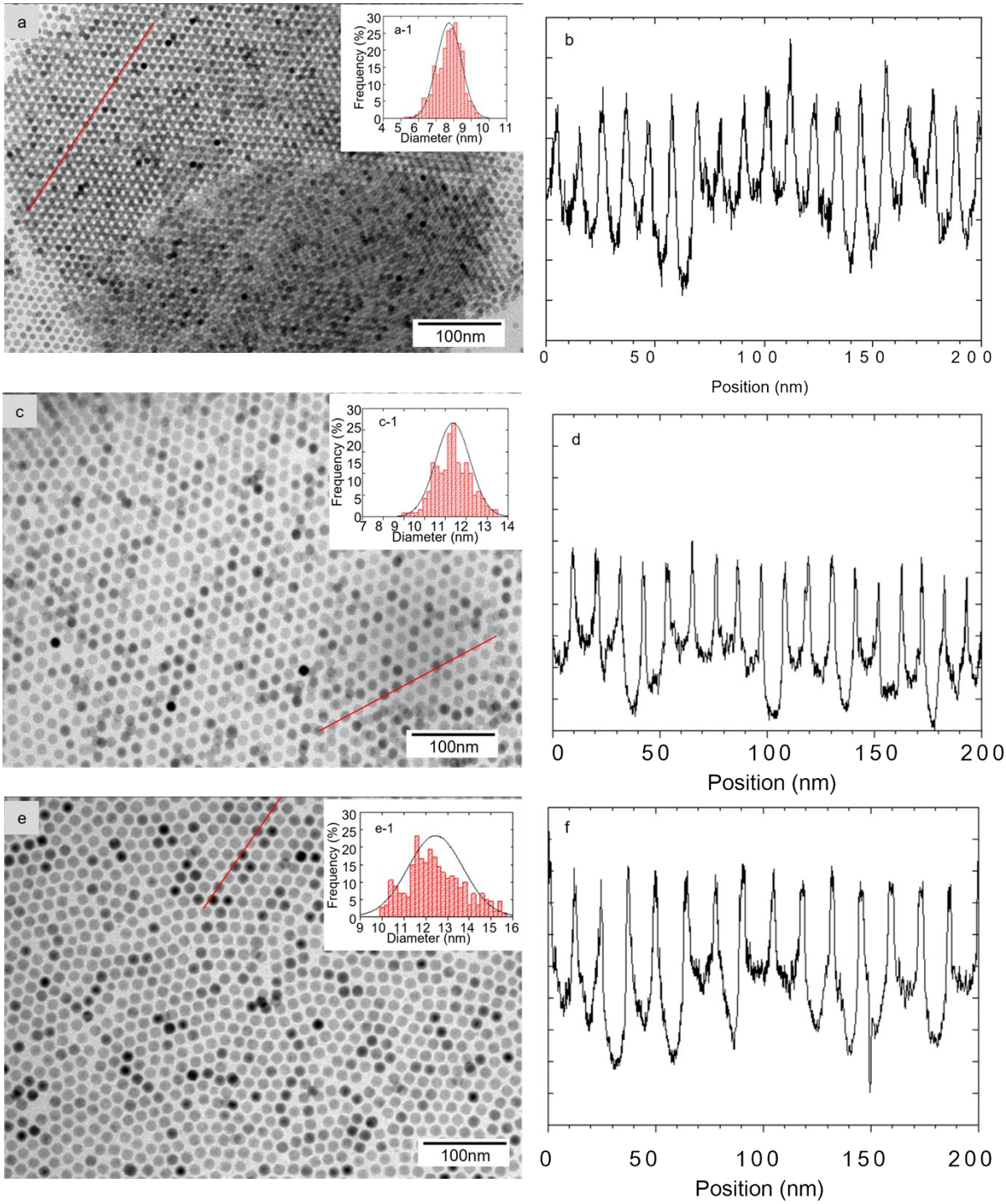

Figure S2. TEM images of γ-Fe_2O_3 NPs of different diameters and contrast profiles made over the red lines, allowing the determination of corresponding effective diameters D_{C-C} *: a) D = 7.9±0.6 nm b)* $D_{c-c} \approx$ *10nm c) D=11.4±0.9 nm d)* $D_{c-c} \approx 13.4$ *nm e) D=12.4±1.0 nm f)* $D_{c-c} \approx 14.2$*nm.*

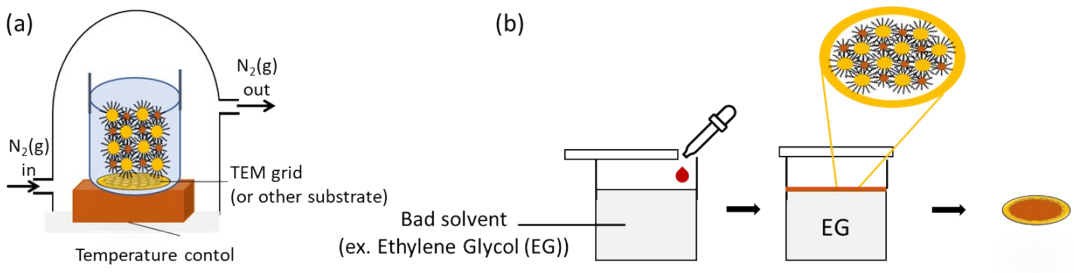

Figure S3: Schemes of preparation methods used for growing ordered binary superlattices.

Table S1 Hildebrand parameters and boiling points of the different solvents used in this study[29–31].

Solvent or (ligands)	Hildebrand solubility parameters ($MPa^{0.5}$)	Dielectric constant	Boiling point (°C)	Evaporation time (hour)
Toluene	18.2	2.38	111	4
Cumene	17.5	2.4	152	5
Hexane	14.9	1.8	68	0.5

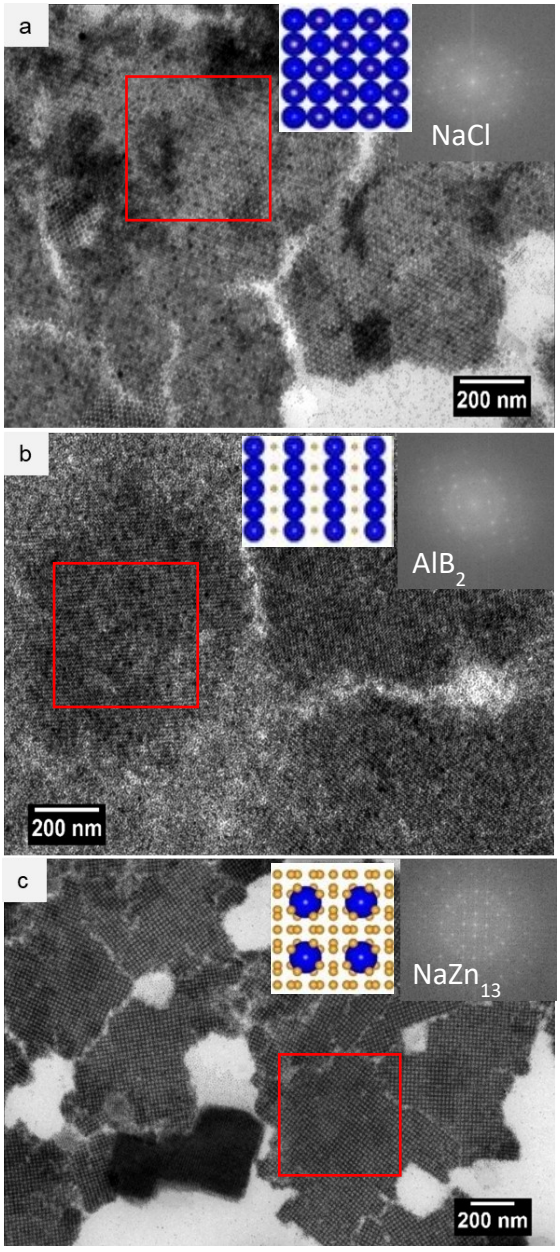

Figure S4. TEM images of BNSLs composed of γ-Fe_2O_3 and Au NPs, with different effective size ratios (γ_{eff}), keeping the other conditions unchanged ([γ-Fe_2O_3]/[Au])=1/4, T_d=50°C), γ_{eff} = (a) 0.45 (b) 0.48 (c) 0.64. Insets: the FFT analysis performed on selected areas (red squares) of the binary superlattices and BNSL structures corresponding to TEM images.

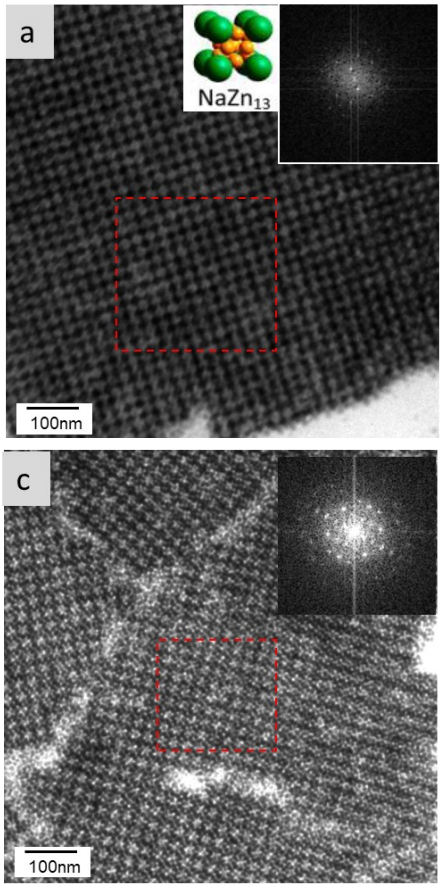

Figure S5. TEM images of $NaZn_{13}$ type binary superlattices formed with 7.9nm γ-Fe_2O_3 and 4.6nm Au NPs with fixed effective size ratio (γ_{eff} =0.64) and deposition temperature Td=50°C by using different solvents a) toluene and b) cumene. Insets: the FFT analysis performed on selected areas (red squares) of the binary superlattices and representation of unit cell of $NaZn_{13}$ type binary structure.

Table S2. Interparticle distance $D_{C\text{-}C}$ between magnetic NPs (γ-Fe_2O_3 NPs) in thin BNSLs and pure γ-Fe_2O_3 NP assemblies.

	Binary superlattices formed with 7.9 nm γ-Fe_2O_3 and 4.6 nm Au NPs	**Pure 7.9 nm γ-Fe_2O_3 NP superlattices**
$\boldsymbol{D_{C\text{-}C}}$	13.8 nm	10 nm
Crystalline structure	$NaZn_{13}$	*fcc*

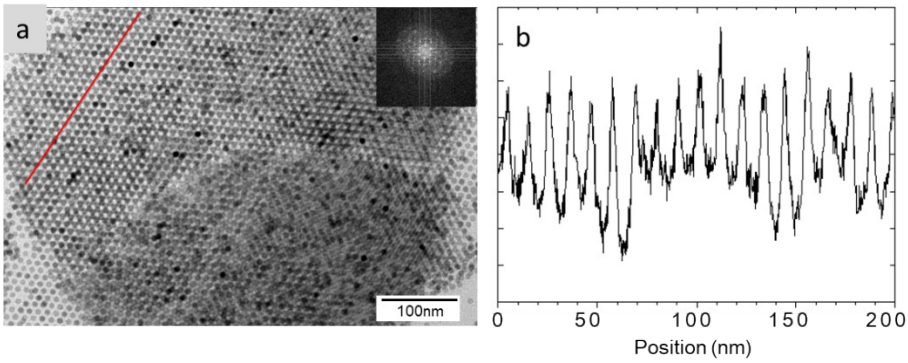

Figure S6. (a) TEM image of thin layers of γ-Fe_2O_3 NPs with their FFT image (inset) and (b) the contrast profile made over the red line, indicating an interparticle distances $D_{C\text{-}C}\approx 10$ nm.

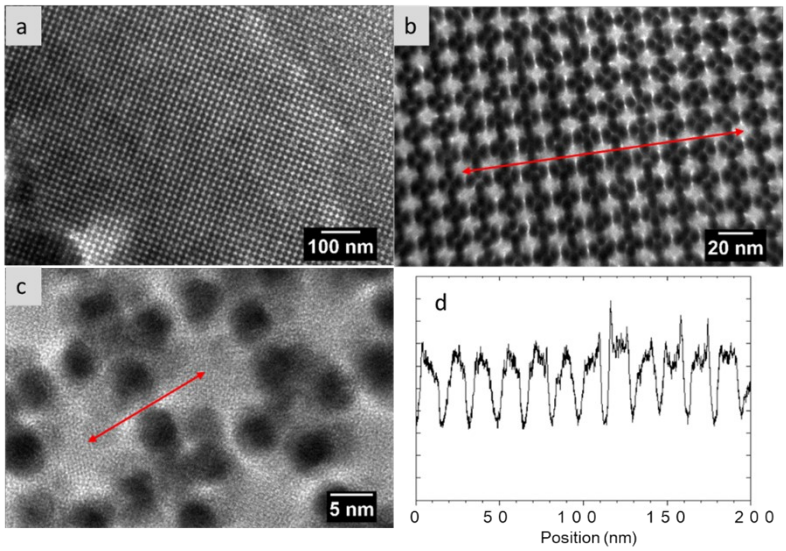

Figure S7. (a-c) HR-TEM images of $NaZn_{13}$ BNSL structure at different magnifications and (d) the contrast profile made over the red line, from (b) indicating an interparticle distances D_{C-C}≈13.8 nm.

Table S3. Comparison of the blocking temperature and the coercivity values obtained by SQUID measurements for pure γ-Fe_2O_3 superlattices and γ-Fe_2O_3 -Au BNSLs. All values are deduced from Figure 6.

	SQUID	
	Blocking temperature, T_b (K)	**Coercivity, H_c (Oe)**
γ-Fe_2O_3 superlattices	84	360
γ-Fe_2O_3-Au BNSLs	76	360